

VSLLaVA: a pipeline of large multimodal foundation model for industrial vibration signal analysis

Qi Li^a, Jinfeng Huang^a, Hongliang He^a, Xinran Zhang^a, Feibin Zhang^{a,*}, Zhaoye Qin^{a,*} and Fulei Chu^a

^aState Key Laboratory of Tribology, Department of Mechanical Engineering, Tsinghua University, Beijing, 100084, P.R. China

ARTICLE INFO

Keywords:

Large language model
Large multimodal model
Expert knowledge
Signal analysis
Vibration signal

ABSTRACT

Large multimodal foundation models have been extensively utilized for image recognition tasks guided by instructions, yet there remains a scarcity of domain expertise in industrial vibration signal analysis. This paper presents a pipeline named VSLLaVA that leverages a large language model to integrate expert knowledge for identification of signal parameters and diagnosis of faults. Within this pipeline, we first introduce an expert rule-assisted signal generator. The generator merges signal provided by vibration analysis experts with domain-specific parameter identification and fault diagnosis question-answer pairs to build signal-question-answer triplets. Then we use these triplets to apply low-rank adaptation methods for fine-tuning the linear layers of the Contrastive Language-Image Pretraining (CLIP) and large language model, injecting multimodal signal processing knowledge. Finally, the fine-tuned model is assessed through the combined efforts of large language model and expert rules to evaluate answer accuracy and relevance, which showcases enhanced performance in identifying, analyzing various signal parameters, and diagnosing faults. These enhancements indicate the potential of this pipeline to build a foundational model for future industrial signal analysis and monitoring.

1. Introduction

Recently, significant advancements have been made in the field of large language models (LLMs). Models like ChatGPT and GPT-4 have shown impressive reasoning skills that rival or even exceed human capabilities [1]. These large language models have revolutionized various domains by integrating text, images, and other data formats, enhancing artificial intelligence's problem-solving abilities. Drawing on the success of LLMs, large vision-language models (LVMs) or large multimodal models (LMMs) have also undergone a transformative evolution [2, 3]. The utilization of these foundation models in numerous fields has resulted in promising outcomes in different categories of subsequent assignments. In the convergence of artificial intelligence, machine learning, and domain-specific applications, LVMs have paved the way for novel opportunities across various fields such as scientific research, engineering, healthcare [4, 5, 6].

The primary objective of LMM is to develop a general-purpose multimodal model capable of following arbitrary instructions and solving various tasks specified by the user which creates a universal vision task interface that allows the model to solve a wide range of tasks, leveraging the synergies from diverse instructions [7]. LMM also enhances the model's interactivity and adaptability, enabling it to follow arbitrary user instructions with high accuracy. Recent advancements of open source LMM, such as LLaVA [8, 9], have demonstrated the enhanced capabilities of these models in image content recognition and reasoning within the domain of vision-language tasks, showcasing superior performance compared to earlier approaches. The development of such general-purpose multimodal models represents a significant step forward in the field, offering powerful tools for solving a wide array of vision tasks with greater flexibility and efficiency.

Currently, LMM possesses general knowledge for universal image recognition but struggles with identifying specialized information, particularly in industrial signal analysis within the prognostics and health management (PHM) field [10]. PHM plays a vital role in ensuring safety and optimizing maintenance and operational costs, with

*Corresponding author: Zhaoye Qin, Feibin Zhang

✉ liq22@tsinghua.org.cn (Q. Li); hjinfeng1991@163.com (J. Huang); danson127hhl@gmail.com (H. He); xinran-z24@mails.tsinghua.edu.cn (X. Zhang); zfbn2008@163.com (F. Zhang); qinzy@mail.tsinghua.edu.cn (Z. Qin); chuf1@mail.tsinghua.edu.cn (F. Chu)

ORCID(s): 0000-0001-7105-2818 (Q. Li); 0000-0003-3892-4594 (Z. Qin)

signal processing and identification being crucial for system monitoring. Traditionally, extracting valuable insights from signals has been a challenging task, requiring advanced signal processing and machine learning technologies. Generic signal analysis methods such as signal modulation and feature extraction are utilized for diagnosis, parameter identification, and fault diagnosis, with techniques like Fourier transform and Hilbert-Huang transform commonly employed [11, 12].

In essence, the current approach to utilizing LMM in PHM has several limitations.

- From the perspective of LMM, lacking specialized signal processing knowledge hinders obtaining outputs that align with operational logic without specific cues, thereby restricting performance in complex signal processing and fault diagnosis.
- In terms of signal analysis and monitoring in PHM, task-specific methods such as parameter identification and pattern recognition are required, lacking a universally applicable interface. Each task is handled individually within a single framework, incorporating task guidance implicitly in model design. The need for designing separate models for parameter identification poses challenges in interacting with signal analysis experts.
- Enabling language to bridge signals to language semantics remains a challenge. The current efforts struggle to establish a direct connection between them due to the heterogeneity in signal and language representations.

To tackle the issue, we introduce VSLLaVA, a LLaVA-style model that incorporates industrial analysis knowledge using a set of signal-question-answer (SQA) triplets discussed between LLM and PHM experts. We then employ LLM and applied low-rank adaptation (Lora) techniques [13] to fine-tune the linear layers of CLIP [14] and the language model. The fine-tuned model is evaluated in partnership with LMM signal experts to gauge the accuracy and relevance of the ground truth answers, showcasing enhanced performance in detecting and analyzing different signal parameters within publicly available models.

The contributions are as follows:

- In order to overcome the lack of expertise in signal analysis within the LLM framework, we introduce the VSLLaVA pipeline. This pipeline incorporates expert knowledge in signal analysis into the SQA generator, combines LLaVA-style tuning, and involves expert-LLM mixed evaluation.
- The SQA generator leverages domain-specific knowledge to produce simulated and real signals along with corresponding expert Q&A pairs. Through efficient fine-tuning, signals and language are aligned in the semantic space.
- By employing a collaborative evaluation approach between experts and LLM, eight different types of signals are validated to show the fine-tuned model significantly enhances knowledge in signal analysis and fault diagnosis, with the potential to pave the way for industrial applications.

The remainder of this paper is organized as follows. Section II provides related works about visual instruction and signal analysis. Section III presents the proposed VSLLaVA pipeline. Section IV describes the experimental setup, results and discussion. Section V draws the conclusion and future works.

2. Related works

2.1. Visual instruction tuning multimodal model

The wide applications of LLM in various fields such as natural language processing and text generation have been well established. However, early LLMs were typically limited to a single modality, which posed significant constraints when dealing with complex, multidimensional signal analysis requirements [15]. To address this challenge, researchers have progressively developed multimodal models, with the integration of visual and textual information being a popular approach. These multimodal models can simultaneously process and comprehend visual and language information, showcasing their potential in more intricate tasks.

The LLaVA series models have gained significant attention. Firstly, liu et al. proposed the attempt to extend instruction grounding to the language-image multimodal domain with an end-to-end trained large multimodal model that connects visual encoders and LLM to achieve universal visual and language understanding, enhancing zero-shot capability for new tasks [8]. Building upon the research on LLaVA, LLaVA v1.5 [9] demonstrated the effectiveness

of using multi-layer perceptrons (MLP) as visual-language connector. A method was proposed to encode images independently by segmenting them into grids, enabling the model to scale to arbitrary resolutions. To further improve the efficiency of fine-tuning LLM models, Luo et al. [16] proposed the use of lightweight modules to connect the image encoder and LLM. This facilitates joint optimization between the two components and includes a routing algorithm to assist LLM in automatically switching between single-modal and multi-modal instructions. Building on Multi-Modal Adapter, the authors introduced a novel multi-modal LLM called LaVIN. The Mixture-of-Modality Adaptation (MMA) and Multi-Modal Training are utilized in this framework. Through MMA, LaVIN is capable of quickly adapting to vision language tasks without the need for extensive pre-training. In parallel, Yin et al. [17] presented an introduction to a multimodal instruction adjustment dataset containing images and point clouds, emphasizing fine-grained information and factual knowledge, along with a detailed construction method. Additionally, a potential Language-Assisted Multi-Modal instruction tuning (MLLM) training framework was proposed to optimize modality expansion, offering baseline models, experimental observations, and analysis. Gao et al. [18] introduced LLaMA-Adapter V2, which is trained using small-scale image-text and instruction data without the need for large-scale multimodal instruction data. The model enhances language instruction following capability by adjusting bias and scale parameters of linear layers. Additionally, it employs joint training by optimizing different parameter sets using image-text paired data and instruction-following data to address interference between image-text alignment and instruction following. Zhang et al. expanded on these concepts with the introduction of the LLaVAR model [19], which aims to enhance the model's understanding of text in images by collecting and leveraging rich textual image data. They discussed how instruction tuning improves the model's generalization ability to unseen tasks. Chen et al. [20] proposed a new method called Position-enhanced Visual Instruction Tuning (PVIT), which integrates additional region-level visual encoders to extend the functionality of MLLMs, facilitating a more detailed understanding of images. They introduced linear projection alignment and end-to-end fine-tuning, along with a region-level instructional data generation scheme to meet the needs of region-level instruction data generation.

However, the studies mentioned above mainly focus on general vision-language tasks and lack application in specific industrial fields. It is important to also consider specialized tasks like analyzing industrial vibration signals as they play a vital role in protecting industrial assets and the safety of operators.

2.2. Industrial vibration signal analysis

Industrial vibration signal analysis is a key technology in the field of PHM. It involves the application of signal processing, machine learning, and deep learning techniques. This analysis can be used for mechanical fault detection/diagnosis, mechanical condition monitoring, etc. [21]. Randall et al. [22] conducted a review on envelope analysis techniques to identify signal and fault characteristic frequencies. Wavelet transform, as discussed by [23], facilitates multi-resolution analysis of non-stationary signals to aid in feature extraction.

Reference [24] utilized Discrete Wavelet Transform as a signal processing method. They computed useful statistical features from the collected signals and employed Correlation-based Feature Selection to identify the optimal features. Subsequently, they classified the data using Random Forest and MLP neural networks. In a study by Ali et al. [25], in 2019, two identical induction motors were subjected to various single and multiple faults (electrical and/or mechanical) in laboratory experiments. They simultaneously measured the stator current and vibration signals of the motors and utilized these signals to develop fault diagnosis methods. The researchers employed Matching Pursuit and Discrete Wavelet Transform as signal processing techniques for feature extraction. Furthermore, they evaluated the performance and suitability of seventeen different classifiers, including Support Vector Machine (SVM), K-Nearest Neighbors, and ensemble algorithms.

In addition to machine learning, specific deep learning modules also contribute to feature learning and end-to-end signal processing. Wang et al. [26] proposed a novel convolutional neural network model, MIMTNet, aimed at enhancing the ability to diagnose bearing faults using multidimensional signal features. Ye et al. [27] introduced a new deep neural network, DMCNet, designed for feature learning from gearbox vibration signals, improving the accuracy and efficiency of fault diagnosis. They proposed a special morphological filtering layer that automatically updates structural elements through opening and closing operations. Ribeiro et al. [28] developed a multi-head one-dimensional convolutional neural network based on multi-channel vibration signals to detect and diagnose six different types of motor faults. Vibration signals were measured using two accelerometers in different directions, with each head independently processing data from each sensor to enhance feature extraction capabilities. Li et al. [29] proposed a new approach called the Enhanced Deep Sparse Autoencoder for diagnosing gear pitting faults with relatively limited raw vibration signal data. This approach combines data augmentation with a deep sparse autoencoder algorithm for fault

diagnosis in gear wear. It uses a sparse autoencoder in deep learning to extract core information from high-dimensional signals and applies data augmentation to expand the dataset, improving the SAE’s ability to detect gear pitting and corrosion faults.

However, these approaches require specific methods for specific tasks and lack the general-purpose interactive capabilities of large multimodal models (LMM). Therefore, there is an urgent need to develop an LMM model for industrial signal processing.

3. VSLLaVA

3.1. The whole pipeline

To bridge the gap between LMMs and industrial vibration signal analysis, we propose VSLLaVA as shown in Fig. 1, a LLaVA-style model enhanced with domain-specific adaptations. We use LLaVA as the base model and apply c techniques to fine-tune the linear layers of CLIP and the language model. The fine-tuned model is then evaluated in collaboration with LMM signal experts to assess answer accuracy and relevance. Our results demonstrate improved performance in identifying and analyzing various signal parameters within open-source models.

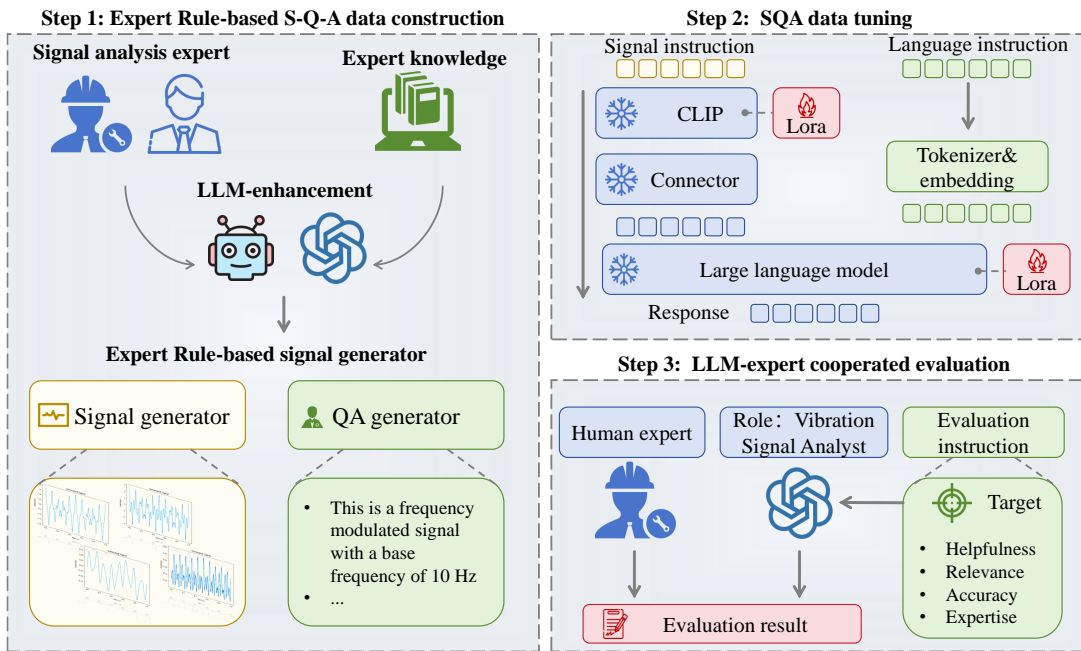


Figure 1: Pipeline of VSLLaVA.

3.2. Expert Rule-based signal generator

In the signal processing field, the community is experiencing a shortage of signal-text pairs due to a lack of relevant knowledge in vibration signal analysis. To address this, we initially establish signal-question-text (SQA) triplets using an expert rule-based signal generator. Drawing from the concept of curriculum learning [30], a machine learning approach that gradually exposes models to increasingly difficult tasks mirroring human learning processes, we can effectively build the basic signal from complex signal in Table 1. Moreover, in industrial signal analysis, we specifically examine signal parameters such as the correlation between harmonic frequencies, the presence of peak frequencies associated with fault features (like those found in bearings of common industrial equipment), and the frequency-based positions of spectral peaks.

By employing the data construction methodology of LLaVA, we have developed eight distinct datasets, as depicted in Table 1, wherein the question-answer pairs are constructed based on domain-specific knowledge encompassing

Table 1
Dataset information.

Dataset name	abbreviation	Equation	Identify parameters
Amplitude modulated signal	AM	$y_{am} = (1 + m \cos(2\pi f_m t)) \cos(2\pi f_c t)$	m, f_m, f_c
Frequency modulated signal	FM	$y_{fm} = \cos(2\pi (f_c t + \Delta f \sin(2\pi f_m t)))$	$f_c, \Delta f, f_m$
AM and FM signal	AMFM	$y_{amfm} = y_{fm} + y_{am}$	$f_c, \Delta f, f_m$
Single harmonic signal	SH	$y_{sh} = A \sin(2\pi f_b t + \phi)$	A, f_b, ϕ
Multiple harmonic signal	MH	$y_{mh} = \sum_i (A_i \sin(2\pi i f_b t + \phi_i)), i = 1, 2, 3, \dots$	A_i, f_b, ϕ_i
Random harmonic signal	RH	$y_{rh} = \sum_i (A_i \sin(2\pi i f_b t + \phi_i)), i \sim \mathcal{N}(\mu_i, \sigma_i^2)$	A_i, f_b, ϕ_i
Combined harmonic signal	CH	$y_{ch} = y_{mh} + y_{rh}$	A_i, f_b, ϕ_i
THU signal	THU	/	/

these parameters and addressing specific tasks like fault diagnosis at THU. The corresponding visual representation of example signals can be observed in Table 2.

These datasets consist of amplitude modulated signals (AM), frequency modulated signals (FM), amplitude modulated and frequency modulated signals (AMFM), single harmonic signals (SH), multiple harmonic signals (MH), random harmonic signals (RH), and combined harmonic signals (CH). The detailed descriptions are as follows.

3.2.1. Single harmonic signal

Firstly the single harmonic signal can be represented as:

$$y_{sh} = A \sin(2\pi f_b t + \phi) \quad (1)$$

where y_{sh} denotes single harmonic signal. A represents the amplitude, indicating the maximum displacement of the vibration. f_b represents the frequency where ϕ denote the phase angle that determines the starting position of the vibration on the time axis.

3.2.2. Multiple harmonic signal

Given the single harmonic signal the multiple harmonic signal can be denoted as:

$$y_{mh} = \sum_i (A_i \sin(2\pi i f_b t + \phi_i)), i = 1, 2, 3, \dots \quad (2)$$

where $i f_b$ represents a composite vibration composed of multiple harmonic frequencies, A_i is the amplitude of the i th harmonic frequency, where i represents the harmonic number, indicating an integer multiple relative to the fundamental frequency f_b . ϕ_i is the phase of the i th harmonic frequency.

3.2.3. Random harmonic signal

The random harmonic signal can be expressed as:

$$y_{rh} = \sum_i (A_i \sin(2\pi i f_b t + \phi_i)), i \sim \mathcal{N}(\mu_i, \sigma_i^2) \quad (3)$$

where A_i and ϕ_i are random variables, and i follows a normal distribution $\mathcal{N}(\mu_i, \sigma_i^2)$.

3.2.4. Combined harmonic signal

The composite waveform formed by the superposition of harmonic wave and random wave can be represented as:

$$y_{ch} = y_{mh} + y_{rh} \quad (4)$$

where y_{ch} represents the total displacement of the combined wave, which is the result of superimposing the harmonic wave.

3.2.5. Frequency modulated signal

The frequency modulated signal can be formulated as follows:

$$y_{fm} = \cos(2\pi(f_c t + \Delta f \sin(2\pi f_m t))) \quad (5)$$

where f_c is the carrier frequency, which is the frequency of the unmodulated signal. Δf is the maximum frequency deviation, indicating the maximum frequency change caused by the modulating signal. f_m is the modulation frequency, determining the rate of change of the modulating signal. The inner function $\sin(2\pi f_m t)$ represents the modulating signal, which is multiplied by Δf and added to the carrier frequency f_c , causing the carrier frequency to vary with time. This equation illustrates the basic form of a frequency modulated wave, where the carrier frequency f_c is influenced by the modulating signal. By multiplying the carrier frequency with the result of the inner function $\sin(2\pi f_m t)$ and adding it to the carrier frequency, a signal with a frequency that varies with time is formed.

3.2.6. Amplitude modulated signal

Amplitude modulation wave can be represented as follows:

$$y_{am} = (1 + m \cos(2\pi f_m t)) \cos(2\pi f_c t) \quad (6)$$

m denotes the modulation index, determining the extent of carrier wave amplitude variation. f_m signifies the modulation frequency, determining the rate of change of the modulation signal. The outer function $\cos(2\pi f_c t)$ represents the carrier signal, while the inner function $1 + m \cdot \cos(2\pi f_m t)$ denotes the impact of the modulation signal on the carrier wave amplitude, causing the carrier amplitude to vary with the modulation signal. This equation illustrates the fundamental form of an amplitude modulation wave, where the carrier wave amplitude $\cos(2\pi f_c t)$ is influenced by the modulation signal, resulting in a signal with amplitude varying over time by multiplying with the inner function $1 + m \cdot \cos(2\pi f_m t)$.

3.2.7. AM and FM signal

Given the y_{am} and y_{fm} , the amplitude-modulated frequency-modulated wave can be obtained via:

$$y_{amfm} = y_{fm} + y_{am} \quad (7)$$

3.2.8. THU signal

Additionally, we employed the self-powered state monitoring dataset based on piezoelectric energy harvesting as shown in Fig. 1 to construct our SQA triplet. This dataset comprises voltage signals from four health conditions (normal, inner race fault, ball fault, and outer race fault). The collected signals were sampled at a frequency of 49600Hz [31].

3.3. SQA data tuning base on LLaVA

In the pipeline illustrated in Fig. 1, two components of LLaVA require fine-tuning using Lora [13]: the vision encoder CLIP and the LLM. Given a pre-trained autoregressive language model $P_{\Phi_a}(X_a|H_q) \circ P_{\Phi_q}(H_q|X_q)$, a pre-trained vision encoder CLIP $P_{\Phi_e}(Z_s|X_s)$, and an MLP connection $P_{\Phi_m}(H_s|Z_s)$, where the MLP connection is used to map image features Z_s into the word embedding space as language embedding tokens H_s , the predicted answer can be obtained by the structured combination of these component as shown in the step 2.

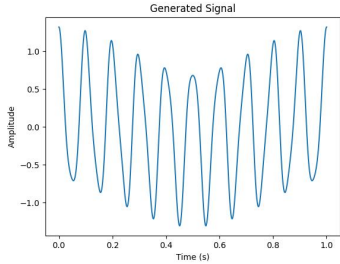
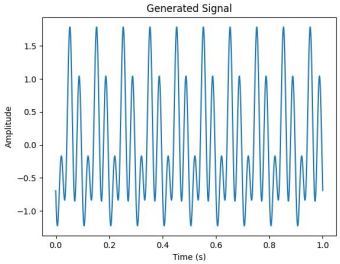
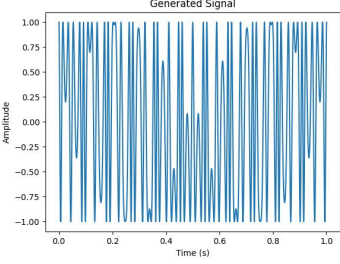
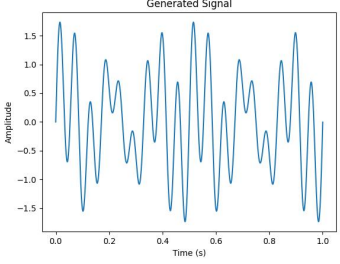
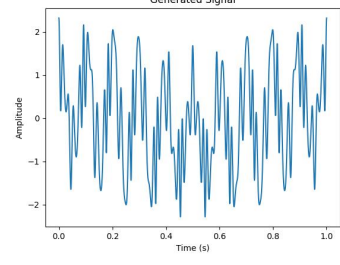
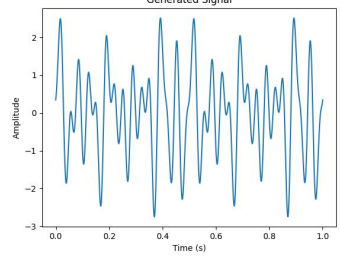
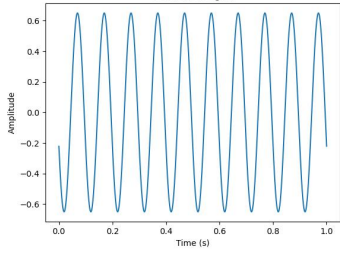
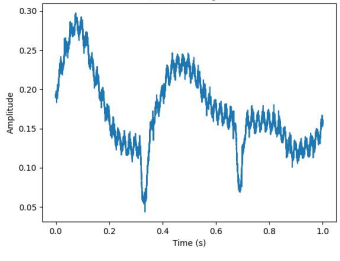
For each signal X_s , we use an expert rule-based signal generator with domain knowledge to generate an SQA group $G = (X_s, X_{q1}, X_{a1}, \dots, X_{qi}, X_{ai}, \dots, X_{qN}, X_{aN})$ to train the VSLLaVA to identify the parameters of the signal for the task. From this group, an instruction pair $\mathbf{X}_{\text{instruct}} = (X_s, X_{q1}, X_{a1})$ is extracted for the first turn, and pairs $\mathbf{X}_{\text{instruct}} = (X_{qi}, X_{ai})$ are used for the remaining turns. Specifically, for a sequence of length N , the probability of the target answers X_a is computed by:

$$P(\mathbf{X}_a | \mathbf{X}_s, \mathbf{X}_{\text{instruct}}) = \prod_{i=1}^N P_{\theta}(X_{ai} | \mathbf{X}_s, \mathbf{X}_{\text{instruct}, <i}, \mathbf{X}_{a, <i}) \quad (8)$$

where $\mathbf{X}_{\text{instruct}, <i}$ and $\mathbf{X}_{a, <i}$ represent the instruction and answer tokens in all turns before the current prediction token X_{ai} , respectively, where θ represents the model parameters.

To achieve effective parameter fine-tuning, which enables adaptation to various tasks without a substantial increase in computational costs, we derive a pre-trained weight matrix $W_0 \in \mathbb{R}^{d \times k}$ from the CLIP and LLM models. weight

Table 2
Signal visualization.

Dataset name	Signal visualization	Dataset name	Signal visualization
AM		MH	
FM		RH	
AMFM		CH	
SH		THU	

matrices in these layers typically have full-rank, then we can constrain its update by representing the latter with a low-rank decomposed into two low-rank matrices A and B :

$$W = W_0 + \Delta W = W_0 + AB \quad (9)$$

with, $A \in \mathbb{R}^{d \times r}$, and $B \in \mathbb{R}^{r \times k}$, where $r \ll d, k$. During the forward pass, the new weight matrix W is used to compute the output:

$$Y = XW = X(W_0 + \Delta W) = XW_0 + XAB \quad (10)$$

Thus, the probability of the target answers can be refined as:

$$P(\mathbf{X}_a | \mathbf{X}_s, \mathbf{X}_{\text{instruct}}) = \prod_{i=1}^N P_{\theta_0 + \Delta\theta}(X_i | \mathbf{X}_s, \mathbf{X}_{\text{instruct}, <i}, \mathbf{X}_{a, <i}) \quad (11)$$

In this work, a parameter-efficient approach of Lora is adopted, where the task-specific parameter increment $\Delta\theta = \Delta\theta(\Theta)$ is encoded by a much smaller set of parameters Θ , with $|\Theta| \ll |\theta_0|$. The task of finding $\Delta\theta$ becomes optimizing over Θ :

$$\max_{\Theta} \sum_G \sum_{i=1}^N \log \left(p_{\theta_0 + \Delta\theta(\Theta)}(X_{a,i} | \mathbf{X}_s, \mathbf{X}_{\text{instruct}, <i}, \mathbf{X}_{a, <i}) \right) \quad (12)$$

where \mathbf{X}_s is the input signal. $\mathbf{X}_{\text{instruct}, <i}$ is the instruction context up to the i -th step. $\mathbf{X}_{a, <i}$ is the sequence of target answer tokens up to the i -th step. $\theta_0 + \Delta\theta(\Theta)$ represents the model parameters, where $\Delta\theta(\Theta)$ is the task-specific parameter adjustment derived from a smaller parameter set Θ . Ultimately, through Lora fine-tuning with SQA, the VSLLaVA model is obtained and then evaluated by LLM and human experts.

3.4. Evaluation of Collaborative Strategy by LLM and human

Evaluating LLM performance can be challenging [32], but automatic evaluation offers a convenient way to assess alignment between predictions and actual outcomes [33]. Some studies have introduced LLM-based evaluation techniques to address subjectivity, automate calculations, and enhance simplicity [34]. In this study, we implement a strategy that involves both LLM and experts for evaluation. Algorithm 1 below presents the specific algorithm utilized in this evaluation process.

Overall, we assign four scores S_a , S_r , S_t , and S_{llm} to represent the absolute score of parameter identification, relative score of parameter identification, similarity of the language and the score from LLM, respectively. Initially, all scores S_a , S_r , S_t , S_{llm} are set to 0 to accumulate individual scores across all samples. N_r and N_a are set for tracking invalid or missing samples, particularly for numerical scores s_a and s_r , where N represents the number of input samples X_a . Additionally, the LLM is initialized with pretrained parameters.

Subsequently, in each sample loop, numerical values are extracted from the actual X_{a_i} and ground truth X_{gt_i} inputs using regular expressions to form parameter sets \mathcal{P}_{a_i} and \mathcal{P}_{gt_i} . After handling outliers to avoid tasks where parameter identification is absent in the text, the corresponding s_a and s_r scores are computed using Eq. 13 and Eq. 14 :

$$s_a = \frac{\sum_{i=1}^n \mathbb{1}(a_i = gt_i)}{n} \times 100\% \quad (13)$$

$$s_r = \frac{\sum_{i=1}^n \max \left(0, 1 - \left| \frac{a_i - gt_i}{a_i + \epsilon} \right| \right)}{n} \times 100\% \quad (14)$$

where $\mathbb{1}$ is the indicator function and n represents the number of parameters extracted from the sentence, a_i and gt_i are parameter in \mathcal{P}_{a_i} and \mathcal{P}_{gt_i} , respectively, and ϵ denotes a stabilizing factor. To assess the language similarity, the words T_a and T_{gt} should be extracted first, and the score of each sample s_t can be calculated as:

$$s_t = \frac{|T_c|}{|T_{gt}|} \times 100\%, T_c = T_a \cap T_{gt} \quad (15)$$

Finally, the comprehensive evaluation score can be achieved by the LLM. By preparing the evaluation input X_{e_i} as Eq. 16 including question X_q , model response X_a , ground truth X_{gt} , role setting X_r evaluation prompt X_p and system prompt X_s , the evaluation input is constructed as

$$X_{e_i} = X_q \oplus X_r \oplus X_a \oplus X_r \oplus X_{gt} \oplus X_{s_i} \quad (16)$$

where \oplus denotes concatenating the content with a separator, then computing the corresponding score through LLM. Finally, the overall average scores S_a , S_r , S_t , and S_{llm} can be calculated.

Algorithm 1 Score calculation via rule and LLM

```

1: function SCORE CALCULATION( $X_{instruct}, X_a, X_{gt}, X_r, X_p, X_s$ )
2:   Initialize  $S_a \leftarrow 0, S_r \leftarrow 0, S_t \leftarrow 0, S_{llm} \leftarrow 0, N_r \leftarrow 0, N_a \leftarrow 0$ 
3:   Initialize sample count  $N \leftarrow$  length of  $X_a$ 
4:   LLM  $P_e$  evaluator initialization
5:   for each sample  $i = 1$  to  $N$  do
6:     Extract parameter set  $\mathcal{P}_{a_i}$  from  $X_{a_i}$  via regular expression ▷ Parameter Extraction
7:     Extract parameter set  $\mathcal{P}_{gt_i}$  from  $X_{gt_i}$  via regular expression
8:     Initialize  $s_{a_i} \leftarrow 0, s_{r_i} \leftarrow 0, s_{t_i} \leftarrow 0, s_{llm_i} \leftarrow 0$ 
9:     if  $\mathcal{P}_{gt_i}$  is empty then ▷ Error Handling
10:       $s_{a_i} \leftarrow -1$ 
11:       $s_{r_i} \leftarrow -1$ 
12:     else if  $\mathcal{P}_{a_i}$  is empty then
13:       $s_{a_i} \leftarrow 0$ 
14:       $s_{r_i} \leftarrow 0$ 
15:     else
16:       Calculate  $s_{a_i}$  using Eq. 13
17:       Calculate  $s_{r_i}$  using Eq. 14
18:     end if
19:     Extract unique words  $T_{a_i}$  from  $X_{a_i}$  ▷ Text extraction
20:     Extract unique words  $T_{gt_i}$  from  $X_{gt_i}$ 
21:     Calculate  $s_{t_i}$  using Eq. 15
22:     Construct  $X_{e_i}$  via Eq.
23:      $s_{llm_i} \leftarrow P_e(X_{e_i})$ 
24:     if then  $s_{a_i} \neq -1$  and  $s_{r_i} \neq -1$ 
25:       Update cumulative scores:  $S_a \leftarrow S_a + s_{a_i}, S_r \leftarrow S_r + s_{r_i}$ 
26:     else
27:       statistic invalid number:  $N_a \leftarrow N_a + s_{a_i}, N_r \leftarrow N_r + s_{r_i}$ 
28:     end if
29:     Update cumulative scores:  $S_t \leftarrow S_t + s_{t_i}, S_{llm} \leftarrow S_{llm} + s_{llm_i}$ 
30:   end for
31:   Calculate average scores:  $S_a \leftarrow \frac{S_a}{N - N_a}, S_r \leftarrow \frac{S_r}{N - N_r}$ 
32:   Calculate average scores:  $S_t \leftarrow \frac{S_t}{N}, S_{llm} \leftarrow \frac{S_{llm}}{N}$ 
33:   return  $S_a, S_r, S_t, S_{llm}$ 
34: end function

```

4. Cases study

4.1. Experiment setting

For ease of implementation and reproducibility, the training and evaluation were conducted using the xtuner [35] and opencompass [36] framework. The relevant parameters for Lora are as indicated in the Table 3. The dataset creates SQA triples using a signal generator with parameters to be identified in different data as shown in Fig. 1. The relevant parameters follow a normal distribution. SQA triples for training, validation, and testing are constructed based on different normal distributions to evaluate the performance of model. The foundation language model is implemented as LLAMA-8B [37]. Besides, we utilized a different LLAMA-8B as an evaluator and employed the following prompt for collaborative optimization with experts and GPT4. The compared method include internlm2[38] using the LLaVA-style tuning and original LLaVA with LLM of LLAMA-8B. All experiments were conducted on servers equipped with 8 Nvidia 4090 GPUs.

4.2. Evaluation prompt

The LLM score is based on GPT4 with human instruction to play the <Vibration Signal Analyst>. The prompt X_p is as follows: "Please assess two results generated by the <Vibration Signal Analyst> for the provided vibration signal

Table 3

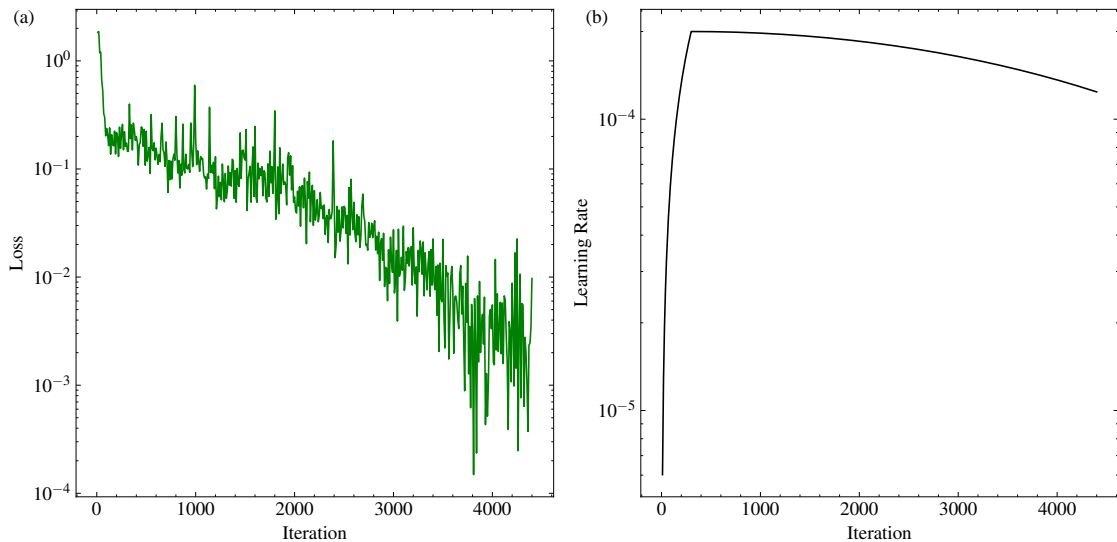
Parameters for tuning the LLM model and visual encoders

Parameter	Value	Parameter	Value
Lora rank of LLM	512	Epochs	10
Alpha of LLM	256	Learning rate	2e-4
Lora rank of visual encoder	64	Warmup ratio	0.03
Alpha of visual encoder	16	Dropout of Lora	0.05

data. The first result represents the ground truth, and the second is produced by a large language model. Evaluate the second result based on its similarity to the first one—the closer the second result is to the ground truth, the higher the score. Additionally, if parameters are identified, assess the accuracy of these parameters, with lower deviation resulting in a higher score. Consider the following factors in your evaluation: helpfulness, relevance, accuracy, and expertise. Each factor should contribute to the overall score, with higher similarity across these dimensions resulting in higher scores. First, output a single line containing only two scores, separated by a space. The first score should reflect the overall similarity to the ground truth across all criteria, and the second score should reflect the accuracy of parameter identification. Afterward, provide a detailed and unbiased explanation of your evaluation, ensuring that the order of presentation does not influence your judgment. Please remember first output a single line containing only two values indicating the score from 1 to 10, which means only two values appear in the first line without word like score, respectively."

4.3. Score result

Fig. 2 displays training process of Lora on the given SQA data, showing that the prediction error significantly decreases with each iteration until reaching $1e-4$. To enhance the training stability, we first employ a linear learning rate warm-up for the initial 3% iterations, and subsequently switch to a cosine annealing learning rate scheduler for the remaining iterations.

**Figure 2:** Loss and Learning rate in the model training.

Based on the scores shown in the Table 4 to 7, it can be observed that after fine-tuning SQA, VSLLaVA outperforms other models in large-scale evaluations, taking into account aspects like helpfulness, relevance, accuracy, and expertise.

Specifically, in Table 4 and Table 5, the evaluation of absolute and relative scores for parameter identification is presented. The scores reflect the performance of the models on various signal types, including SH, MH, RH, CH, AM, FM, AMFM, THU, FM. It can be observed that in the task of parameter identification, the VSLLaVA-llama3 method achieves the best results in S_q . Since absolute scores require a perfect match for scoring, the overall score is lower than

Table 4
Evaluation score S_a according to absolute score (%).

	LLaVA-internlm2	LLaVA-llama3	VSLLaVA-llama3
SH	18.08	20.13	38.93
MH	25.46	22.60	47.39
RH	40.40	36.36	44.52
CH	23.94	25.27	38.29
AM	15.10	18.00	37.10
FM	11.10	11.20	26.70
AMFM	19.56	18.72	36.75
THU	35.83	34.67	66.67
Average	24.50	24.01	42.54

Table 5
Evaluation score S_r according to relative score (%).

	LLaVA-internlm2	LLaVA-llama3	VSLLaVA-llama3
SH	15.65	18.95	56.94
MH	36.56	39.24	60.19
RH	29.97	27.81	53.27
CH	28.55	30.34	58.32
AM	27.09	23.25	70.37
FM	27.10	25.02	61.02
AMFM	40.84	36.54	63.42
THU	20.21	23.86	66.67
Average	28.71	28.47	60.85

Table 6
Evaluation score S_l according to language score (%).

	LLaVA-internlm2	LLaVA-llama3	VSLLaVA-llama3
SH	59.64	59.24	63.95
MH	49.34	47.47	80.36
RH	63.16	61.86	62.39
CH	48.23	46.88	84.74
AM	56.09	56.56	71.72
FM	57.26	56.68	84.84
AMFM	41.45	41.62	77.10
THU	58.45	56.80	84.38
Average	53.59	52.79	76.08

the relative score. It is noticeable that the accuracy of parameter identification for AM and FM signals is relatively lower. However, the proposed method, by incorporating relevant knowledge, improves accuracy by around 20% for AM and FM signals, and by around 30% for real THU signals. Similarly, the proposed method also demonstrates the best performance in Table 5.

In addition to parameter identification, we are also concerned about the quality of the descriptive text. The S_t in Eq. 15 is used to evaluate the similarity between the prediction and the ground truth. It can be observed that for complex vibration signals, especially mixed signals like MH, CH, modulated signals like FM, and actual experimental signals like THU, the proposed method exhibits the highest relevance in text descriptions, leading to an improvement of approximately 35%.

Additionally, to reduce the subjectivity of expert rule-based evaluation methods, we have also employed an LLM agent to assess both the ground truth and predicted responses. The results, as shown in Table 7, indicate that under the guidance of prompt words, the LLM acts as a professional Vibration Signal Analyst, evaluating the predicted responses

Table 7

Evaluation score S_{IIm} according to LLAMA3-8B with the prompt of Vibration signal Analyst.

	LLaVA-internlm2	LLaVA-llama3	VSLLaVA-llama3
SH	6.92	7.26	7.33
MH	6.91	7.07	7.34
RH	6.98	7.23	7.50
CH	6.38	6.95	7.62
AM	6.63	7.02	7.56
FM	6.81	7.26	7.70
AMFM	6.64	6.65	7.13
THU	6.35	7.00	7.45
Average	6.70	7.05	7.45

based on the requirements and ground truth. Overall, the model trained with VSLLaVA has achieved higher evaluation scores.

4.4. Response example

Finally, specific examples can be seen in Table 8 to Table 15. The provided tables present responses from three language models—VSLLaVA-llama3, LLaVA-llama3, and LLaVA-internlm2—compared to ground truth on various signal types: AM, FM, AMFM, SH, MH, RH, CH, and THU. The analysis focuses on the accuracy, detail, and relevance of each model’s response, along with their ability to correctly interpret and describe the signals. Through comparing the results, we can observe that while other models tend to ramble on about unknown areas, in the industrial field, we expect the responses to be precise without any ambiguous information. We need formatting that clearly shows the output format. On the other hand, our model not only accurately identified the relevant parameters but also presented the results succinctly and directly, following the style of SQA accurately.

For the AM signal in Table 8, VSLLaVA-llama3 delivers a precise and accurate description that matches the ground truth, whereas LLaVA-llama3 and LLaVA-internlm2 provide general but less relevant explanations, failing to identify the amplitude modulation characteristic. In the case of the FM signal in Table 9, VSLLaVA-llama3 again excels with an accurate identification of the modulation type, while LLaVA-llama3 incorrectly interprets the signal as random noise, and LLaVA-internlm2 offers a correct but nonspecific response.

For the AMFM signal in Table 10, VSLLaVA-llama3 accurately captures the dual modulation, distinguishing itself from LLaVA-llama3, which incorrectly focuses on signal amplitude without recognizing the modulation coupling, and LLaVA-internlm2, which provides only a general periodic description. When analyzing the SH signal Table 11, VSLLaVA-llama3 accurately identifies the signal’s characteristics, including its period and phase, while LLaVA-llama3 makes a notable error in estimating the period, and LLaVA-internlm2 gives an incomplete but correct response.

In the case of the MH signal in Table 12, VSLLaVA-llama3 demonstrates superior understanding by correctly identifying the multi-harmonic nature and relevant parameters, while LLaVA-llama3 misinterprets the signal as artificially generated, and LLaVA-internlm2 offers a basic description lacking in detail. For the RH signal, VSLLaVA-llama3 accurately describes the complex composition of random frequencies, in contrast to LLaVA-llama3 and LLaVA-internlm2, which provide general sinusoidal descriptions without addressing the signal’s randomness.

The analysis of the CH signal in Table 14 shows that VSLLaVA-llama3 correctly identifies the combined harmonic nature, whereas LLaVA-llama3 makes a critical error by suggesting the signal is generated by a Gaussian process, and LLaVA-internlm2 fails to recognize the signal’s complexity. Finally, for the THU signal in Table 15, VSLLaVA-llama3 accurately identifies the signal’s fault condition and recording frequency, outperforming LLaVA-llama3, which inaccurately suggests artificial generation, and LLaVA-internlm2, which provides a generic description without recognizing the signal’s specific characteristics.

Across all signal types, VSLLaVA-llama3 consistently delivers the most accurate and relevant responses, closely aligning with the ground truth. LLaVA-llama3 and LLaVA-internlm2 often provide correct but less specific or relevant answers, with LLaVA-llama3 occasionally making significant errors in signal interpretation. The results highlight VSLLaVA-llama3’s superior understanding of complex signal characteristics, making it the most reliable model for these tasks.

Table 8
The response example of AM

Model	Response
VSLLaVA-llama3	This is an amplitude modulated signal with a carrier frequency of 10 Hz.
LLaVA-llama3	A notable feature of the signal in the image is its oscillatory nature, as it appears to be a sine wave. This type of signal is commonly used in various applications, such as electronics, telecommunications, and signal processing, due to its periodic and smooth nature. The sine wave can be represented mathematically by the equation $y = A \sin(2 \pi x / T)$, where A is the amplitude, x is the time, and T is the period of the oscillation. In the image, the sine wave has an amplitude of 1, which means it oscillates between -1 and 1.
LLaVA-internlm2	The signal has a sinusoidal pattern, which is a smooth, wavelike shape that repeats over time. This type of signal can represent various physical phenomena, such as sound or light waves, and is often used in mathematical models and simulations. In the image, the signal is represented by a graph that plots the value of the signal over time, with the x-axis representing time and the y-axis representing the amplitude of the signal. The sinusoidal pattern can be seen as the signal oscillates between positive and negative values, creating a wave-like motion.
Groundtruth	This is an amplitude modulated signal with a carrier frequency of [10] Hz.

5. Conclusion

Large multimodal foundation models have been widely applied to image recognition tasks guided by instructions, but their application in industrial signal analysis remains limited due to a lack of domain-specific expertise. This paper introduces VSLLaVA, a pipeline designed to bridge this gap by incorporating expert guidance into Large Multimodal Models for signal analysis. The pipeline includes an expert rule-assisted signal generator, which combines insights from vibration analysis experts with domain-specific parameter identification and fault diagnosis question-answer pairs. These elements are integrated with large language models to create signal-question-answer sets for further optimization and training.

Using LLaVA as the base model, we employ low-rank adaptation techniques to fine-tune the linear layers of contrastive language-image pretraining (CLIP) and the language model. The fine-tuned model is evaluated in collaboration with LLM and rule of signal experts, focusing on answer accuracy and relevance. The results demonstrate notable improvements in identifying and analyzing various signal parameters, highlighting the potential of this pipeline to serve as a foundational model for future advancements in industrial signal analysis and monitoring.

Future work will include expanding the dataset and creating a more comprehensive benchmark to facilitate a more holistic evaluation. Additionally, we aim to pre-train the signal modality encoder using SQA triplets.

6. Acknowledgements

This work was supported in part by the National Nature Science Foundation of China under Grants 11972204 and the Science Center for Gas Turbine Project (Grant No. P2022-B-III-002-001)

References

- [1] OpenAI, GPT-4 Technical Report, arXiv 4 (2023) 1–100. arXiv:2303.08774.
URL <http://arxiv.org/abs/2303.08774>
- [2] Huang, Visual instruction tuning towards general-purpose multimodal model: A survey. arXiv:2312.16602[cs].
URL <http://arxiv.org/abs/2312.16602>
- [3] K. Han, Y. Wang, H. Chen, X. Chen, J. Guo, Z. Liu, Y. Tang, A. Xiao, C. Xu, Y. Xu, Z. Yang, Y. Zhang, D. Tao, A Survey on Vision Transformer, IEEE Transactions on Pattern Analysis and Machine Intelligence 45 (1) (2023) 87–110. arXiv:2012.12556, doi:10.1109/TPAMI.2022.3152247.
- [4] J. Pan, Large language model for molecular chemistry 3 (1) 5–5. doi:10.1038/s43588-023-00399-1.
URL <https://www.nature.com/articles/s43588-023-00399-1>
- [5] S. Gilbert, H. Harvey, T. Melvin, E. Vollebregt, P. Wicks, Large language model AI chatbots require approval as medical devices 29 (10) 2396–2398. doi:10.1038/s41591-023-02412-6.
URL <https://www.nature.com/articles/s41591-023-02412-6>

Table 9

The response example of FM

Model	Response
VSLLaVA-llama3	This is a frequency modulated signal with a base frequency of 10 Hz.
LLaVA-llama3	A notable feature of the signal in the image is that it appears to be generated by a random process. This is evident from the fact that the signal consists of a series of random blue and white lines, which do not seem to follow any specific pattern or trend. This type of signal is often referred to as a "generalized signal" or "generalized noise," and it is commonly used in various fields such as signal processing, communication systems, and data analysis.
LLaVA-internlm2	The signal in the graph has a repeating pattern, which is a characteristic of a sinusoidal function. This type of function is often used to model periodic phenomena, such as sound or light waves. The presence of such a pattern implies that the underlying process generating the signal has a periodic nature.
Groundtruth	This is a frequency modulated signal with a base frequency of [13] Hz.

Table 10

The response example of AMFM

Model	Response
VSLLaVA-llama3	This is a coupled FM-AM signal with a carrier frequency of 11 Hz.
LLaVA-llama3	A notable feature of the signal in the image is that it has a very large amplitude. This suggests that the signal is strong and likely to have a significant impact on whatever system it is a part of. The large amplitude could indicate that the signal is important for the proper functioning of the system, or it could be indicative of an error or anomaly that needs to be addressed.
LLaVA-internlm2	The signal in the image is a periodic, oscillating pattern that repeats over time. This type of signal can be represented by a sinusoidal function, which is a mathematical model of a periodic wave. The sinusoidal function can be used to describe the behavior of various real-world phenomena, such as sound and light waves, as well as other types of periodic oscillations.
Groundtruth	This is a coupled FM-AM signal with a carrier frequency of [16] Hz.

Table 11

The response example of SH

Model	Response
VSLLaVA-llama3	This is a simple harmonic periodic signal. In the time-domain waveform, the period of this signal is [0.1] seconds, and the phase is 3.77 degree
LLaVA-llama3	A notable feature of the signal in the image is that it is a sine wave, which is a type of continuous waveform that oscillates between positive and negative values. This type of signal is commonly used in various fields, such as electrical engineering, telecommunications, and signal processing. The sine wave in the image has a period of 1 second, which means that it completes one cycle of oscillation every second.
LLaVA-internlm2	The signal on the graph has a repeating pattern, which indicates that it is a periodic signal. This type of signal can be represented by a mathematical function with a sinusoidal component, such as a sine or cosine function. The periodic nature of the signal implies that it will continue to oscillate with the same pattern over time.
Groundtruth	This is a simple harmonic periodic signal. In the time-domain waveform, the period of this signal is 0.1 seconds, and the phase is 3.49 degree

- [6] Y. Liu, H. Duan, Y. Zhang, B. Li, S. Zhang, W. Zhao, Y. Yuan, J. Wang, C. He, Z. Liu, K. Chen, D. Lin, MMBench: Is Your Multi-modal Model an All-around Player?, arXiv (April) (2023). arXiv:2307.06281.
URL <http://arxiv.org/abs/2307.06281>
- [7] J. Huang, J. Zhang, A survey on evaluation of multimodal large language models (Aug. 2024). arXiv:2408.15769.
- [8] H. Liu, C. Li, Q. Wu, Y. J. Lee, Visual instruction tuning. arXiv:2304.08485 [cs].
URL <http://arxiv.org/abs/2304.08485>
- [9] H. Liu, C. Li, Y. Li, Y. J. Lee, Improved baselines with visual instruction tuning. arXiv:2310.03744 [cs].
URL <http://arxiv.org/abs/2310.03744>

Table 12

The response example of MH

Model	Response
VSLLaVA-llama3	This is a multi-harmonic periodic signal, specifically a non-simple harmonic periodic signal. The period of this signal is 0.1 seconds. In the frequency spectrum of this signal, the base frequency (1x harmonic) is 10 Hz.
LLaVA-llama3	A notable feature of the signal in the image is that it appears to be a generated signal, rather than a naturally occurring one. This is evident from the fact that the signal is described as a "generalized signal," which suggests that it may have been artificially created or manipulated for a specific purpose. Additionally, the signal is shown on a graph, which further supports the idea that it is not a naturally occurring signal but rather one that has been intentionally created or analyzed.
LLaVA-internlm2	The signal on the graph has a repeating pattern, which indicates that it is a periodic signal. This type of signal can be represented by a mathematical function with a sinusoidal component, such as a sine or cosine function. The presence of such a pattern implies that the signal may have a regular, predictable behavior that can be analyzed and modeled using mathematical techniques.
Groundtruth	This is a multi-harmonic periodic signal, specifically a non-simple harmonic periodic signal. The period of this signal is [0.1] seconds. In the frequency spectrum of this signal, the base frequency (1x harmonic) is [10] Hz.

Table 13

The response example of RH

Model	Response
VSLLaVA-llama3	This is a random harmonic signal, composed of multiple superimposed sinusoidal waves with random frequencies.
LLaVA-llama3	A notable feature of the signal in the image is its oscillatory nature. The signal consists of a series of peaks and troughs, which indicates that it is oscillating between positive and negative values. This type of signal is commonly observed in various fields, such as physics, engineering, and telecommunications. The oscillatory nature of the signal can provide valuable information about the underlying system or process that generated it
LLaVA-internlm2	The signal in the image is a periodic, wavy pattern that oscillates between positive and negative values. This type of signal is often generated by a sinusoidal function, which can be represented by the equation $y(t) = A * \sin(B(t - C)) + D$, where A is the amplitude, B is the angular frequency, C is the phase shift, and D is the vertical shift. The period of the signal is determined by the value of B, and the frequency is determined by the value of $1/B$. In the given image, the vertical shift is positive, as the signal oscillates above the horizontal axis.
Groundtruth	This is a random harmonic signal, composed of multiple superimposed sinusoidal waves with random frequencies.

- [10] E. Zio, Prognostics and Health Management (PHM): Where are we and where do we (need to) go in theory and practice, *Reliability Engineering and System Safety* 218 (October 2021) (2022). doi:10.1016/j.ress.2021.108119.
- [11] P. Zhou, S. Chen, Q. He, D. Wang, Z. Peng, Rotating machinery fault-induced vibration signal modulation effects: A review with mechanisms, extraction methods and applications for diagnosis 200 110489. doi:10.1016/j.ymsp.2023.110489.
URL <https://linkinghub.elsevier.com/retrieve/pii/S0888327023003977>
- [12] X. Qin, C. Peng, G. Zhao, Z. Ju, S. Lv, M. Jiang, Q. Sui, L. Jia, Full life-cycle monitoring and earlier warning for bolt joint loosening using modified vibro-acoustic modulation, *Mechanical Systems and Signal Processing* 162 (May 2021) (2022) 108054. doi:10.1016/j.ymsp.2021.108054.
URL <https://doi.org/10.1016/j.ymsp.2021.108054>
- [13] E. Hu, Y. Shen, P. Wallis, Z. Allen-Zhu, Y. Li, S. Wang, L. Wang, W. Chen, Lora: Low-Rank Adaptation of Large Language Models, *ICLR 2022 - 10th International Conference on Learning Representations* (2022) 1–26 arXiv:2106.09685.
URL <http://arxiv.org/abs/2106.09685>
- [14] A. Radford, J. W. Kim, C. Hallacy, A. Ramesh, G. Goh, S. Agarwal, G. Sastry, A. Askell, P. Mishkin, J. Clark, G. Krueger, I. Sutskever, Learning transferable visual models from natural language supervision. arXiv:2103.00020[cs].
URL <http://arxiv.org/abs/2103.00020>

Table 14

The response example of CH

Model	Response
VSLLaVA-llama3	This is a combined harmonic signal, which is composed of a multi-harmonic signal and a random harmonic signal. In the frequency spectrum of this signal, the base frequency: 10 Hz.
LLaVA-llama3	A notable feature of the signal in the image is that it appears to be generated by a Gaussian process. This type of signal is known for its smooth and continuous nature, and it is often used in signal processing and machine learning applications. In the image, the signal is represented as a plot of amplitude versus time, with the x-axis representing time and the y-axis representing the amplitude of the signal. The signal is characterized by its smooth and continuous nature, which is indicative of a Gaussian process.
LLaVA-internlm2	The signal on the graph has a repeating pattern, which indicates that it is a periodic signal. This type of signal can be represented by a mathematical function with a sinusoidal component, such as a sine or cosine function. The presence of such a pattern implies that the signal may have a regular, predictable behavior that can be analyzed and modeled using mathematical techniques.
Groundtruth	This is a combined harmonic signal, which is composed of a multi-harmonic signal and a random harmonic signal. In the frequency spectrum of this signal, the base frequency: [10] Hz.

Table 15

The response example of THU

Model	Response
VSLLaVA-llama3	This is a THU signal representing a bearing with a condition classified as outer fault. The signal was recorded at a frequency of 1hz.
LLaVA-llama3	A notable feature of the signal in the image is that it is a generated signal, which means that it has been artificially created rather than being a naturally occurring phenomenon. This is evident from the fact that the signal is described as a "generalized signal" and "generalized signal curve," suggesting that it is not a real-world signal but rather a representation or simulation of one. The signal is also described as a "generalized signal curve" and "generalized signal curve plot," indicating that it is a graphical representation of the signal rather than the actual signal itself.
LLaVA-internlm2	The signal in the image is an example of a sine wave, which is a continuous, periodic curve that oscillates between a maximum and a minimum value. In this case, the maximum value is 1 and the minimum value is 0. The sine wave can be described by its amplitude, frequency, and phase shift. The amplitude is the distance from the midpoint to the maximum or minimum value, which in this case is 0.5. The frequency is the number of oscillations per unit time, and the phase shift is the horizontal displacement of the sine wave from the vertical axis. In the image, the sine wave appears to have a phase shift of 0, as it starts at the vertical axis.
Groundtruth	This is a THU signal representing a bearing with a condition classified as outer fault. The signal was recorded at a frequency of 1hz.

- [15] L. Fan, L. Li, Z. Ma, S. Lee, H. Yu, L. Hemphill, A Bibliometric Review of Large Language Models Research from 2017 to 2023, *ACM Transactions on Intelligent Systems and Technology* (2024) 1–36 [arXiv:2304.02020](https://arxiv.org/abs/2304.02020), doi:10.1145/3664930.
URL <http://arxiv.org/abs/2304.02020>
- [16] G. Luo, Y. Zhou, T. Ren, S. Chen, X. Sun, R. Ji, Cheap and Quick: Efficient Vision-Language Instruction Tuning for Large Language Models, *37th Conference on Neural Information Processing Systems (NeurIPS 2023)* (2023).
- [17] Z. Yin, J. Wang, J. Cao, Z. Shi, D. Liu, M. Li, X. Huang, Z. Wang, L. Sheng, L. Bai, J. Shao, W. Ouyang, LAMM: Language-Assisted Multi-Modal Instruction-Tuning Dataset, Framework, and Benchmark, *37th Conference on Neural Information Processing Systems (NeurIPS 2023)* (2023).
- [18] P. Gao, J. Han, R. Zhang, Z. Lin, S. Geng, A. Zhou, W. Zhang, P. Lu, C. He, X. Yue, H. Li, Y. Qiao, LLaMA-Adapter V2: Parameter-Efficient Visual Instruction Model, *arXiv:2304.15010 [cs]* (Apr. 2023). doi:10.48550/arXiv.2304.15010.
URL <http://arxiv.org/abs/2304.15010>
- [19] Y. Zhang, R. Zhang, J. Gu, Y. Zhou, N. Lipka, D. Yang, T. Sun, LLaVAR: Enhanced Visual Instruction Tuning for Text-Rich Image Understanding, *arXiv:2306.17107 [cs]* (Feb. 2024). doi:10.48550/arXiv.2306.17107.
URL <http://arxiv.org/abs/2306.17107>

- [20] C. Chen, R. Qin, F. Luo, X. Mi, P. Li, M. Sun, Y. Liu, Position-Enhanced Visual Instruction Tuning for Multimodal Large Language Models, arXiv:2308.13437 [cs] (Sep. 2023). doi:10.48550/arXiv.2308.13437.
URL <http://arxiv.org/abs/2308.13437>
- [21] J. Lee, F. Wu, W. Zhao, M. Ghaffari, L. Liao, D. Siegel, Prognostics and health management design for rotary machinery systems - Reviews, methodology and applications, *Mechanical Systems and Signal Processing* 42 (1-2) (2014) 314–334. doi:10.1016/j.ymsp.2013.06.004.
URL <http://dx.doi.org/10.1016/j.ymsp.2013.06.004>
- [22] R. B. Randall, J. Antoni, Rolling element bearing diagnostics-A tutorial, *Mechanical Systems and Signal Processing* 25 (2) (2011) 485–520. doi:10.1016/j.ymsp.2010.07.017.
URL <http://dx.doi.org/10.1016/j.ymsp.2010.07.017>
- [23] R. Yan, Z. Shang, H. Xu, J. Wen, Z. Zhao, X. Chen, R. X. Gao, Wavelet transform for rotary machine fault diagnosis:10 years revisited, *Mechanical Systems and Signal Processing* 200 (January) (2023) 110545. doi:10.1016/j.ymsp.2023.110545.
URL <https://doi.org/10.1016/j.ymsp.2023.110545>
- [24] M. Hosseinpour-Zarnaq, M. Omid, E. Biabani-Aghdam, Fault diagnosis of tractor auxiliary gearbox using vibration analysis and random forest classifier, *Information Processing in Agriculture* 9 (1) (2022) 60–67. doi:10.1016/j.inpa.2021.01.002.
URL <https://linkinghub.elsevier.com/retrieve/pii/S2214317321000020>
- [25] M. Z. Ali, M. N. S. K. Shabbir, X. Liang, Y. Zhang, T. Hu, Machine Learning-Based Fault Diagnosis for Single- and Multi-Faults in Induction Motors Using Measured Stator Currents and Vibration Signals, *IEEE Transactions on Industry Applications* 55 (3) (2019) 2378–2391, conference Name: IEEE Transactions on Industry Applications. doi:10.1109/TIA.2019.2895797.
URL <https://ieeexplore.ieee.org/abstract/document/8627962>
- [26] Y. Wang, M. Yang, Y. Li, Z. Xu, J. Wang, X. Fang, A Multi-Input and Multi-Task Convolutional Neural Network for Fault Diagnosis Based on Bearing Vibration Signal, *IEEE Sensors Journal* 21 (9) (2021) 10946–10956, conference Name: IEEE Sensors Journal. doi:10.1109/JSEN.2021.3061595.
URL <https://ieeexplore.ieee.org/abstract/document/9360815>
- [27] Z. Ye, J. Yu, Deep morphological convolutional network for feature learning of vibration signals and its applications to gearbox fault diagnosis, *Mechanical Systems and Signal Processing* 161 (2021) 107984. doi:10.1016/j.ymsp.2021.107984.
URL <https://linkinghub.elsevier.com/retrieve/pii/S0888327021003794>
- [28] R. F. R. Junior, I. A. D. S. Areias, M. M. Campos, C. E. Teixeira, L. E. B. Da Silva, G. F. Gomes, Fault detection and diagnosis in electric motors using 1d convolutional neural networks with multi-channel vibration signals, *Measurement* 190 (2022) 110759. doi:10.1016/j.measurement.2022.110759.
URL <https://linkinghub.elsevier.com/retrieve/pii/S0263224122000616>
- [29] X. Li, J. Li, Y. Qu, D. He, Semi-supervised gear fault diagnosis using raw vibration signal based on deep learning, *Chinese Journal of Aeronautics* 33 (2) (2020) 418–426. doi:10.1016/j.cja.2019.04.018.
URL <https://www.sciencedirect.com/science/article/pii/S1000936119302018>
- [30] Y. Zhou, X. Wang, H. Chen, X. Duan, W. Zhu, Intra- and Inter-Modal Curriculum for Multimodal Learning, *MM 2023 - Proceedings of the 31st ACM International Conference on Multimedia* (2023) 3724–3735doi:10.1145/3581783.3612468.
- [31] L. Zhang, F. Zhang, Z. Qin, Q. Han, T. Wang, F. Chu, Piezoelectric energy harvester for rolling bearings with capability of self-powered condition monitoring, *Energy* 238 (2022) 121770. doi:10.1016/j.energy.2021.121770.
URL <https://doi.org/10.1016/j.energy.2021.121770>
- [32] Y. Chang, X. Wang, J. Wang, Y. Wu, L. Yang, K. Zhu, H. Chen, X. Yi, C. Wang, Y. Wang, W. Ye, Y. Zhang, Y. Chang, P. S. Yu, Q. Yang, X. Xie, A Survey on Evaluation of Large Language Models, *ACM Transactions on Intelligent Systems and Technology* 15 (3) (2024) 1–27. arXiv:2307.03109, doi:10.1145/3641289.
URL <http://arxiv.org/abs/2307.03109>
- [33] L. Yang, S. Zhang, L. Qin, Y. Li, Y. Wang, H. Liu, J. Wang, X. Xie, Y. Zhang, Glue-x: Evaluating natural language understanding models from an out-of-distribution generalization perspective, arXiv preprint arXiv:2211.08073 (2022).
- [34] Y. Chen, R. Wang, H. Jiang, S. Shi, R. Xu, Exploring the use of large language models for reference-free text quality evaluation: An empirical study, arXiv preprint arXiv:2304.00723 (2023).
- [35] InternLM/xtuner, original-date: 2023-07-11T03:18:13Z.
URL <https://github.com/InternLM/xtuner>
- [36] open-compass/opencompass, original-date: 2023-06-15T12:42:58Z.
URL <https://github.com/open-compass/opencompass>
- [37] A. Dubey, A. Jauhri, e. a. Pandey, The llama 3 herd of models. arXiv:2407.21783 [cs].
URL <http://arxiv.org/abs/2407.21783>
- [38] Z. Cai, M. Cao, e. a. Chen, InternLM2 technical report (Mar. 2024). arXiv:2403.17297.